Supporting Information

Pico-Molar Electrochemical Detection of Ciprofloxacin at Composite Electrodes

Vikram Singh[a], *Sabine Kuss*[a]*

[a]University of Manitoba, Department of Chemistry, Winnipeg R3T 2N2, Canada.

*Corresponding author Email: sabine.kuss@umanitoba.ca

Experimental Section

1. Materials and Chemicals:

Ciprofloxacin and carbon nanotubes (CNTs; OD; 10-30 nm, L; 5-15 μm) were purchased from Sigma Adrich (>95%). Sodium sulphate ($NaNO_3$; > 98%; Britain) and sodium hydroxide (NaOH) were obtained from Fischer Scientific (Belgium). All chemicals were used as received.

Preparation of Oxygen-functionalized Carbon Nanotubes (OCNTs): Oxygen functionalization was achieved by acid treatment[1]. In short, 0.4 g of the as procured CNTs were added in a mixture of 100 ml of H_2SO_4 and HNO_3 (3:1; v/v) at 50 °C. Further, the mixture was continuously and vigorously stirred for 5 h, followed by washing multiple times with nanopure water until the pH became neutral. The obtained product was filtered and dried overnight in an oven at 80 °C. The formed product was used after grinding in a mortal-pestle.

Modification of Electrodes: An OCNTs slurry was prepared by initially dispersing 2.5 mg of OCNTs in 40 μL of isopropanol (IPA) in an Eppendorf tube, followed by sonicating for 20 minutes [23]. To obtain a fine suspension the slurry was further sonicated for 1 h after adjusting its volume to 1.0 ml using nanopure water (>18 MΩ). A GCE was modified by drop-casting 20 μL of the OCNTs slurry onto the GCE, followed by drying in an oven at 45 °C.

Electro-deposition of polydopamine (PDA): In order to enhance the sensitivity of the composite sensor, a thin layer of the conductive PDA was electro-deposited on a glassy carbon electrode, decorated with OCNTs. The chronoamperometric measurements were performed at a potential of 1.0 V (*vs.* Ag/AgCl) in the PBS electrolyte solution, containing 5 mM of dissolved dopamine at room temperature for different intervals of time (30-120 sec) [4]. It is important to note that the polymerization of dopamine is highly sensitive towards light exposure and therefore all measurements were performed under dark conditions.

Electro-deposition of Ag nanoparticles (Ag-NPs): The Ag-NPs electro-deposition was achieved by applying a double-pulse technique, where two potentials (growth and nucleation potential) were selectively chosen based on cyclic voltammetry collected in nitrogen purged 3 mM $AgNO_3$ [5]. Ag-NPs were electro-deposited on a GCE, containing OCNTs-PDA. Optimal electro-deposition conditions were determined by varying several deposition parameters (growth potential, nucleation potential, growth time, nucleation time, and pulse deposition cycles) and collecting the respective response towards the oxidation of ciprofloxacin in the voltammograms. Electro-deposition was controlled by selectively altering the potential of both growth and nucleation with specific duration, one at a time. The obtained Ag-NPs were then comprehensively characterized by SEM, TEM, and XPS analyses.

Physical characterization: The morphological analysis of the OCNTs, PDA and Ag-NPs structures was performed using an FEI Nova NanoSEM 450 microscope. SEM imaging for electrodes was performed by preparing the samples on screen printed electrodes (SPE). TEM and EDX measurements were performed on an FEI Talos F200X microscope at an accelerating voltage of 80 keV.

The X-ray photoelectron spectroscopy (XPS) measurements were performed in an ultra-high vacuum (UHV) set-up using a Kratos Axis Ultra DLD spectrometer. A high-resolution VG ESCA-3 Mk II spectrometer, operating at 15 kV, 15 mA, and 10^{-9} mbar base pressure was employed for the analysis. All XPS measurements were performed at a pass energy of 20 eV in fixed transmission mode, resulting in an overall energy resolution of 0.20 eV, whereby a charge neutralizer was applied to recompense the subsequent charging effects. High resolution spectra were recorded for C1s, O1s, N1s, and Ag3d.

Electrochemical measurements: All electrochemical measurements were performed using a modular SP-200 potentiostat/galvanostat (EC-lab software; BioLogic, France). A three-electrode set-up was employed in a single-chambered glass electrochemical cell inside a faraday cage (Custom production, University of Santa Barbara, CA, USA). A glassy carbon electrode (GCE; BASI, USA) served as a working electrode (WE). A platinum wire functioned as a counter electrode (CE) and an Ag/AgCl/3M KCl (BASI, USA) was used as a reference electrode (RE). Prior to each measurement, the working electrode (GCE) was carefully polished with different grades of alumina slurry (1.0, 0.3, and 0.05 μm; Buehler, USA) on nylon polishing cloths (Struers, Germany). In order to maintain consistency and to avoid any variation in the capacitive currents, a single GCE was used for all electrochemical measurements. The scan rate analysis was performed by varying it form 5 mV s^{-1} to 125 mV s^{-1}. The background current was subtracted in

the Origin using *peak analyser* function in *user defined* baseline mode. The obtained peak current value was plotted against the scan rate.

All electrochemical measurements were performed using nanopure water (>18 MΩ cm) at room temperature and ambient pressure.

Electrochemical methods, such as cyclic voltammetry (CV), square wave voltammetry (SWV), and chronoamperometry (CA) have been used to characterize and detect trace amounts of ciprofloxacin. All CVs were conducted in a potential range of 0.6 to 1.5 V (*vs.* Ag/AgCl) at a fixed scan rate of 50 mV s^{-1} (except for the scan rate variation analysis). All SWV measurements were performed at a pulse height of 5 mV for 100 ms and a step height of 10 mV after every 100 ms each, in their respective potential windows. For better comparison, background correction was performed in origin for SWV data collected.

Tap water analysis:

The entire tap water analysis were performed in regular tap water after adding a known amount of Cip (powder) followed by sonicating it for 20 minutes. However, the solubility of Cip is very low in the tap water, and therefore we could not see any current signal even in the presence of 0.5 mM Cip. The low solubility of Cip was evidenced by the formation of crystalline product on the edges of the electrochemical cell when the sample was monitored closely (Cip solution in tap water) for few hours. However, when the pH of the same solution (0.5 mM Cip in tap water) was adjusted to 5.80, a significant improvement in the current signal was observed. This could be due to the improved solubility and conductivity of the tap water. Besides the current signal, no trace of the crystalline product was detected on the walls of the electrochemical cell as was the case before.

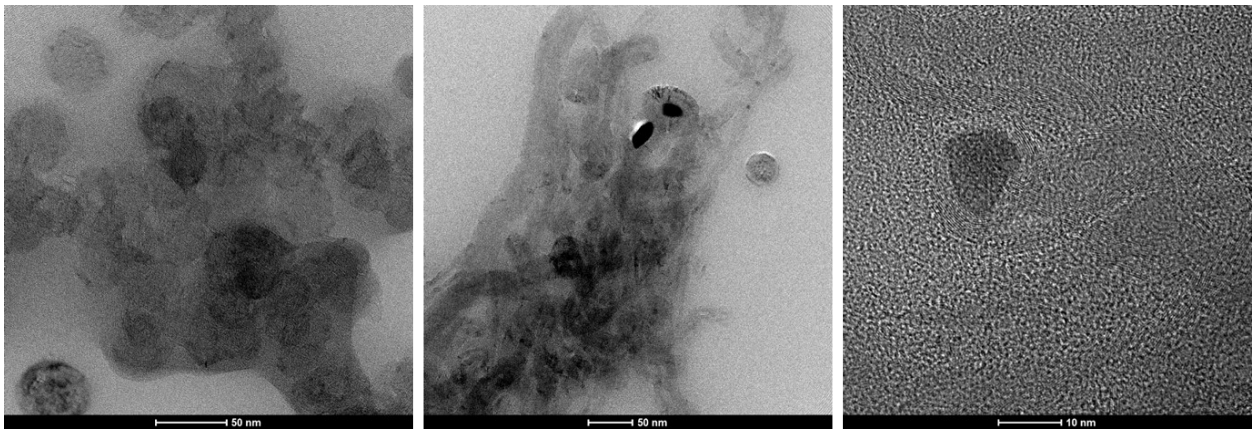

Fig. S1. TEM and HR-TEM imaging of the OCNTs-PDA-Ag sensor.

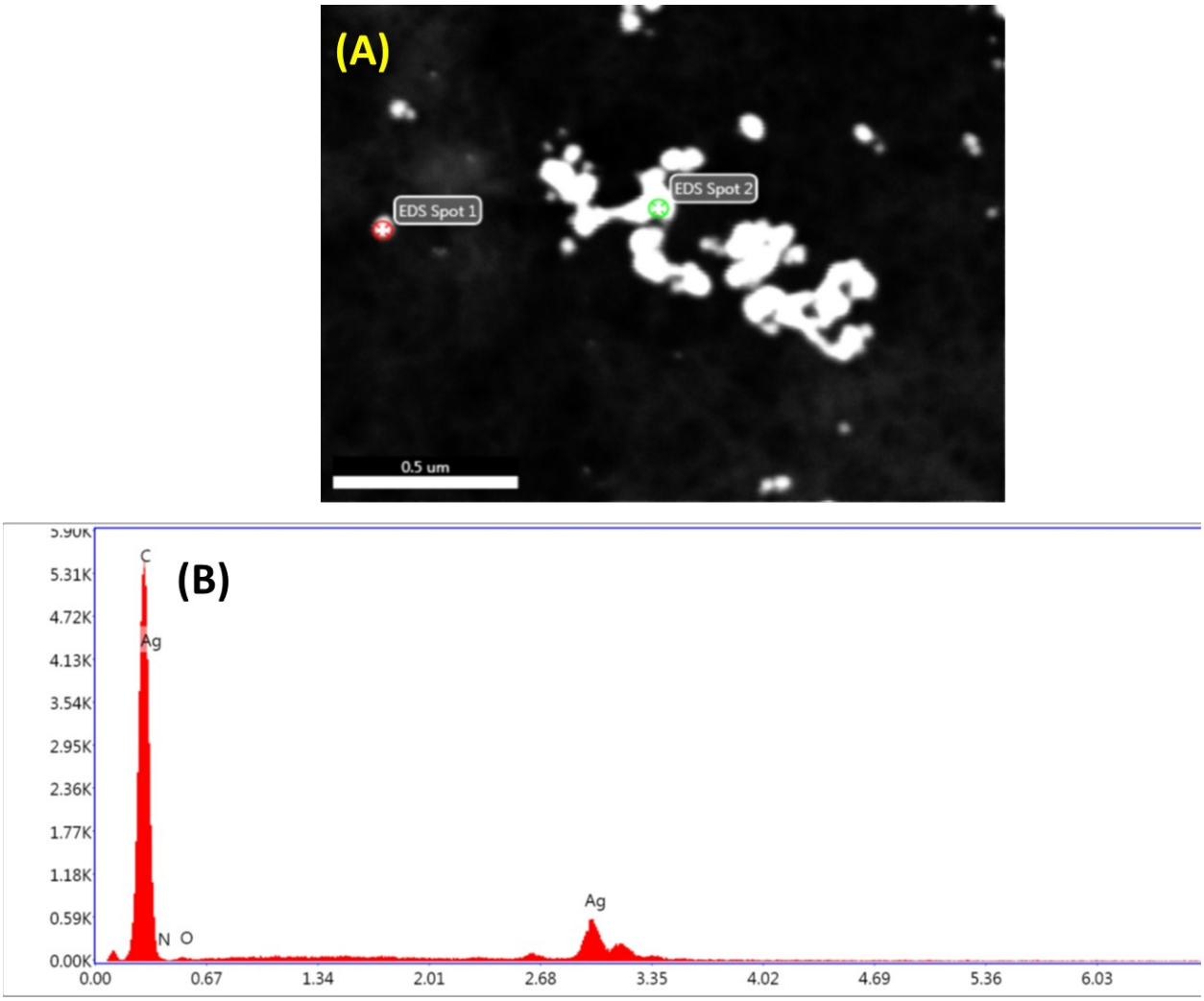

Fig. S2. EDX shows the respective elements in the OCNTs-PDA-Ag sensor.

Table S1: Elemental composition at the selected area in Figure S2- S3.						
	Carbon		**Oxygen**		**Silver**	
Sample	EDX	XPS	EDX	XPS	EDX	XPS
OCNTs	97.4	98.1	2.6	1.8	--	--
OCNTs-PDA-Ag	94.8	94.5	2.0	2.1	3.1	3.0

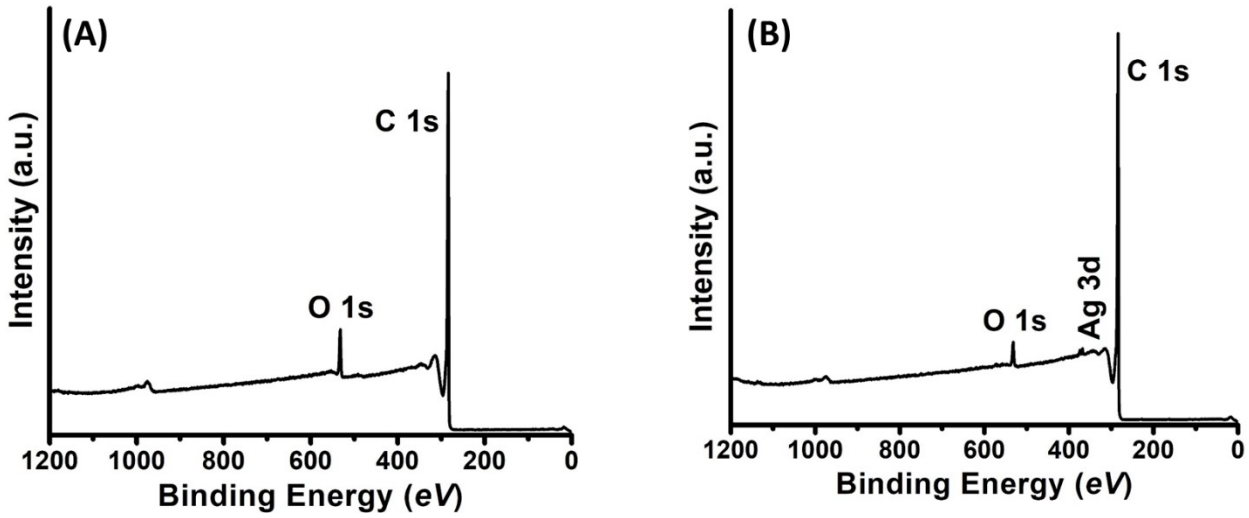

Fig. S3. XPS survey spectra for (A) OCNTs, and (B) OCNTs-PDA-Ag biosensor.

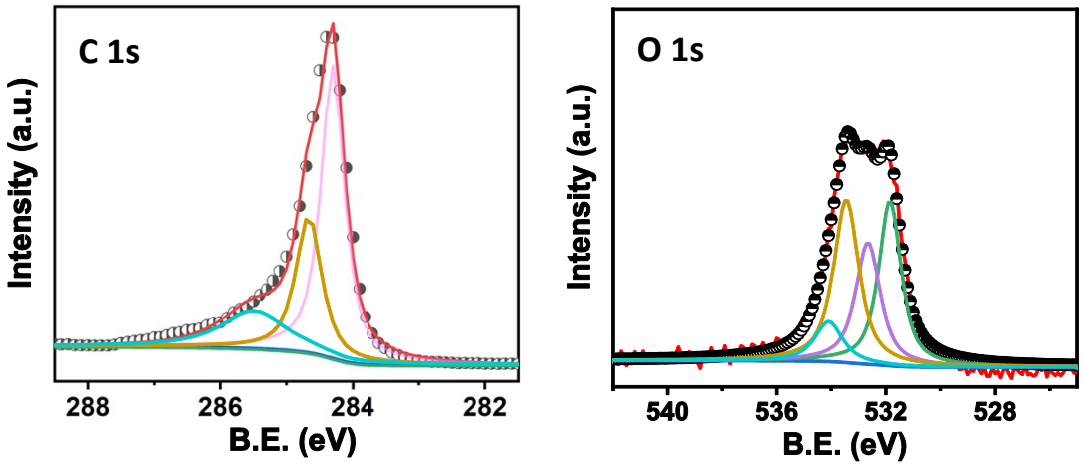

Fig. S4. XPS de-convoluted spectra of C 1s, and O 1s of OCNTs.

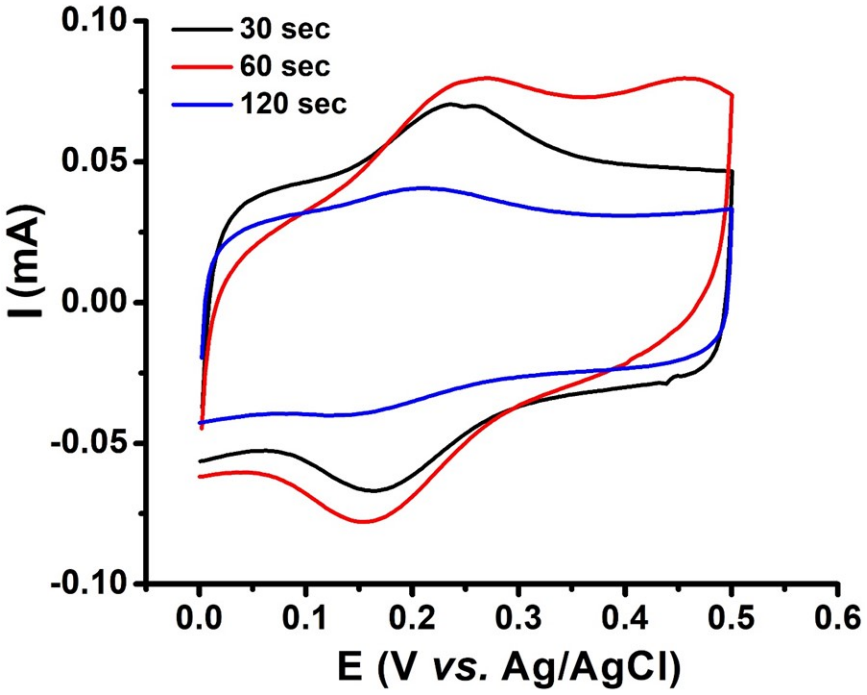

Fig. S5. Cyclic voltammogram showing the reduction peak for polydopamine (PDA) after the polymerization of 30, 60 and 120 s.

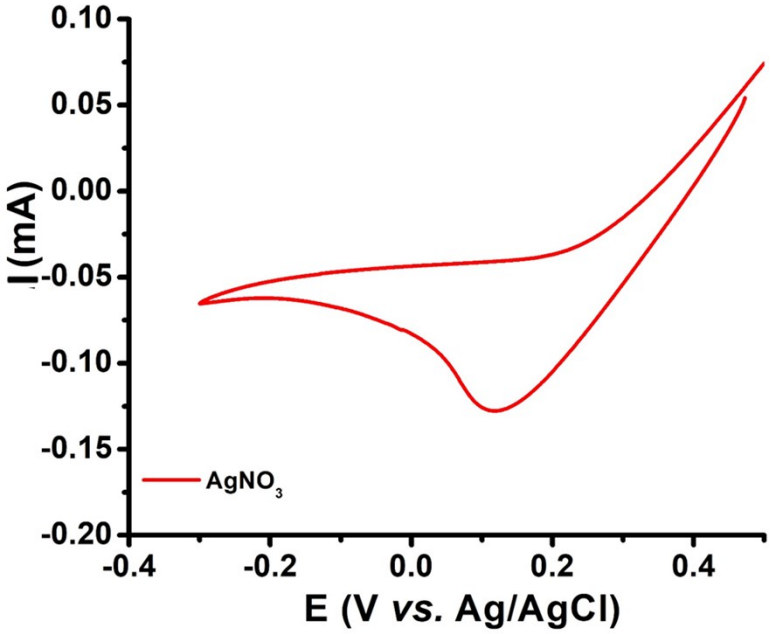

Fig. S6. Cyclic voltammogram at the OCNTs-PDA coated GCE, collected in 3 mM of $AgNO_3$ solution.

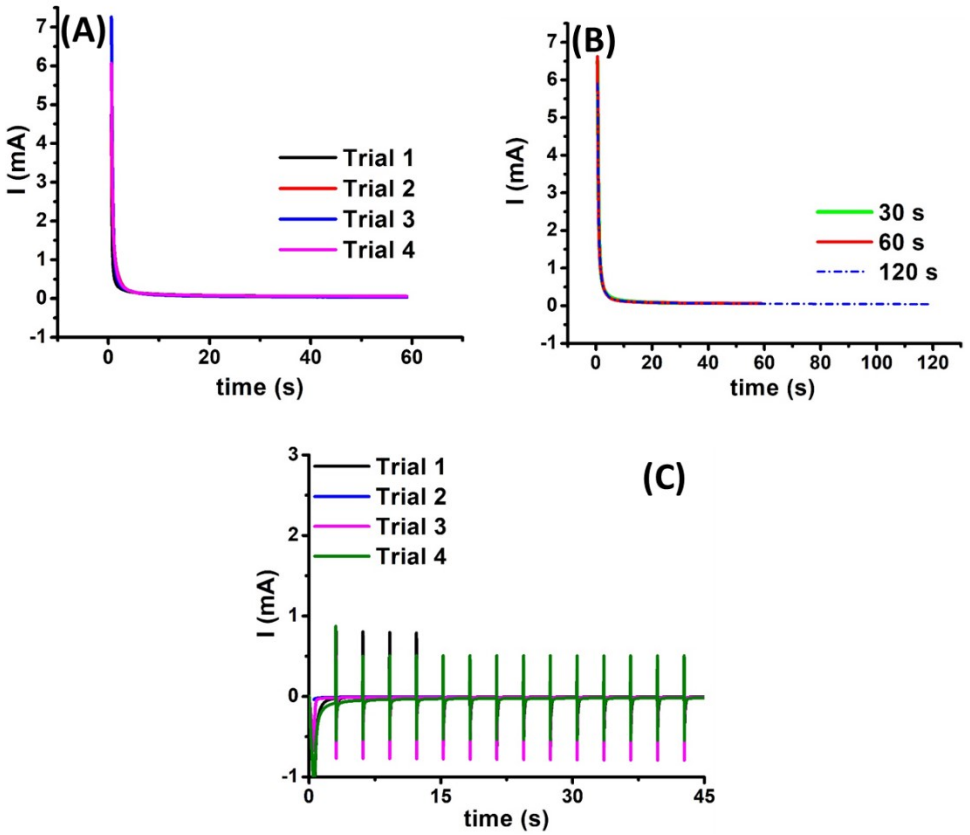

Fig. S7. Fig. 1. (A) Chronoamperograms for electropolymerization of dopamine at 1.0 V for different durations of 30, 60 and 120 s, and (B) Chronoamperograms of different trials for dopamine electrodeposition at 1 V for 60s to ascertain reproducibility. (C) Double-pulse chronoamperometric measurements collected in 3 mM $AgNO_3$ aqueous solution to electrodeposite the Ag-NPs.

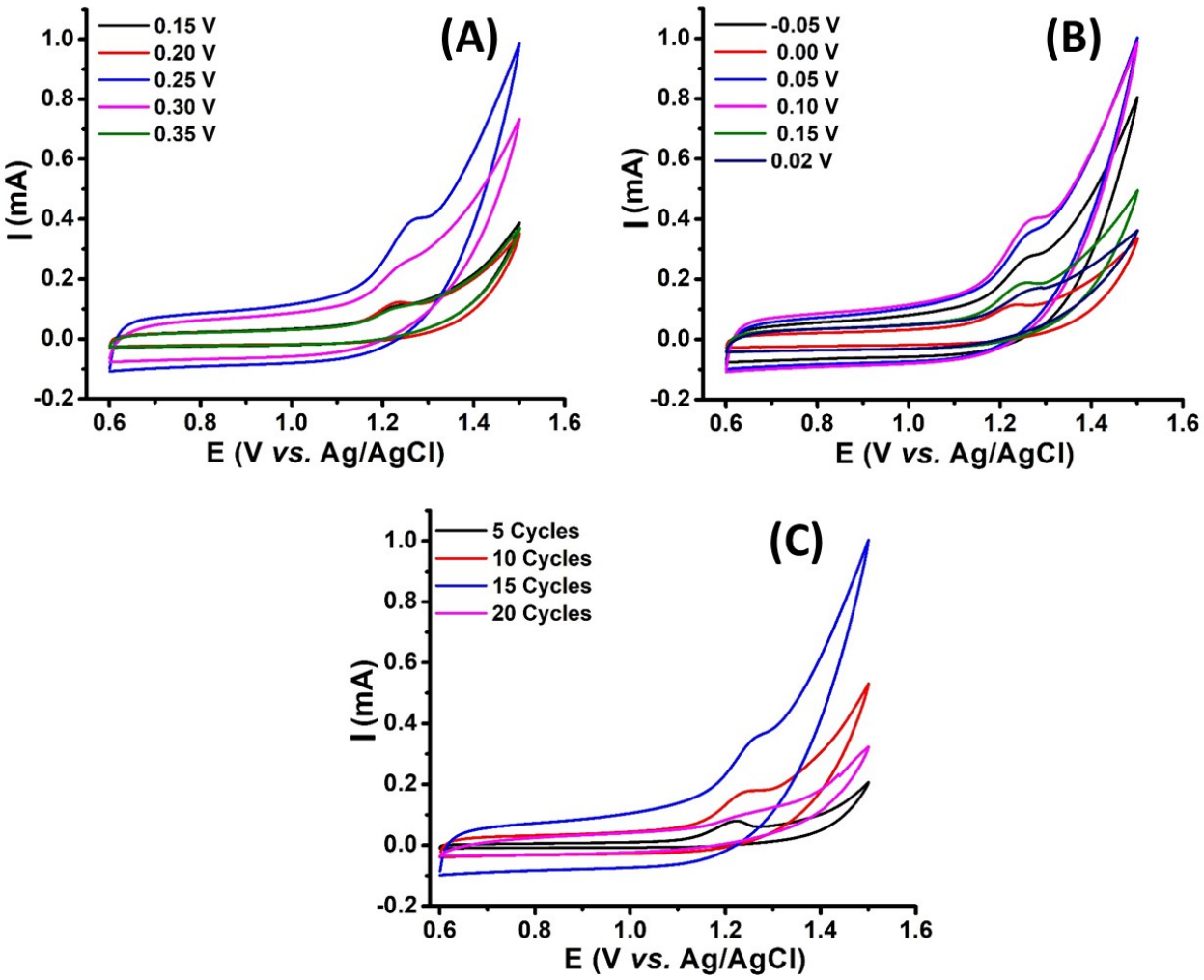

Fig. S8. Cyclic voltammograms collected during the optimization of various deposition parameters, (A) nucleation potential, (B) growth potential and (C) number of deposition cycles.

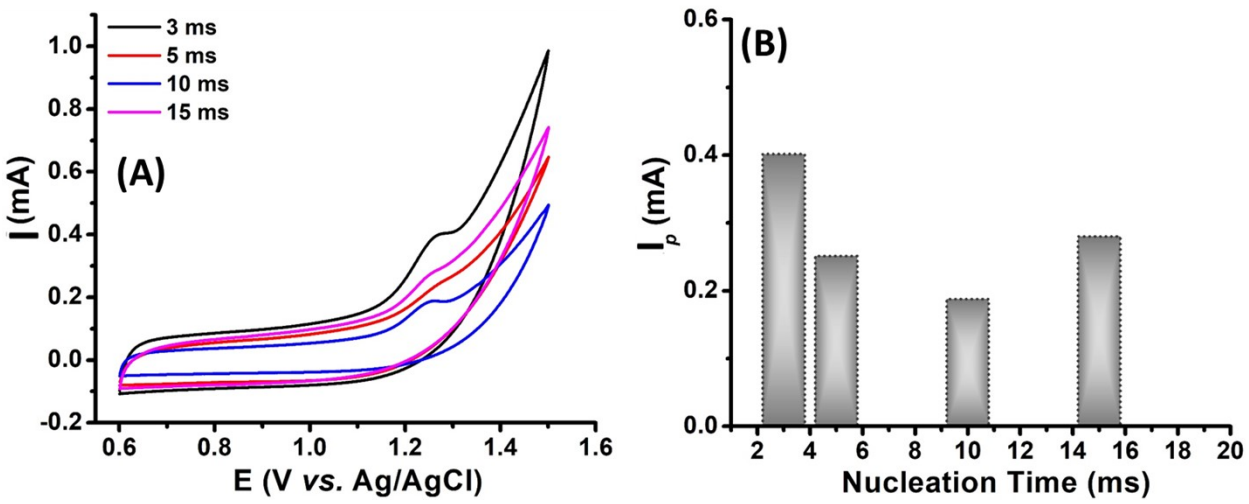

Fig. S9. Optimization of nucleation time (A) cyclic voltammogram and (B) bar graph represent the obtained response towards the detection of Cip.

Table S2: Comparison of Different Methods for the Determination of Ciprofloxacin.			
Electrode	**Technique**	**Limit of Detection; LOD (nM)**	**Ref**
ds-DNA -BDD	SWV	440	[6]
Porous-Nafion-MWCNT/ BDD	DPV	5	[7]
TiO_2 sol	CV	108	[8]
AuNPs/Cyclodextrin/RGO/GC	DPV	2.7	[9]
β-CD/MWCNT/GC		50	[10]
NH2-UiO-66/ RGO	ASV	6.67	[11]
Au/C3N4/GN	SWV	420	[12]
OCNT-PDA-Ag	**SWV**	**0.75 (0.1 M $NaNO_3$) 5 (Tap Water)**	**Present Work**

Table S3: Comparison of electrochemical sensing with standard detection techniques.		
Sensing Techniques	**Detection limit**	**Ref**
HPLC	0.51~64.8 µM	[13]
Mass spectroscopy	5 nM	[14]
OCNTs-PDA-Ag Electrochemical sensor	**750 pM**	**Present work**

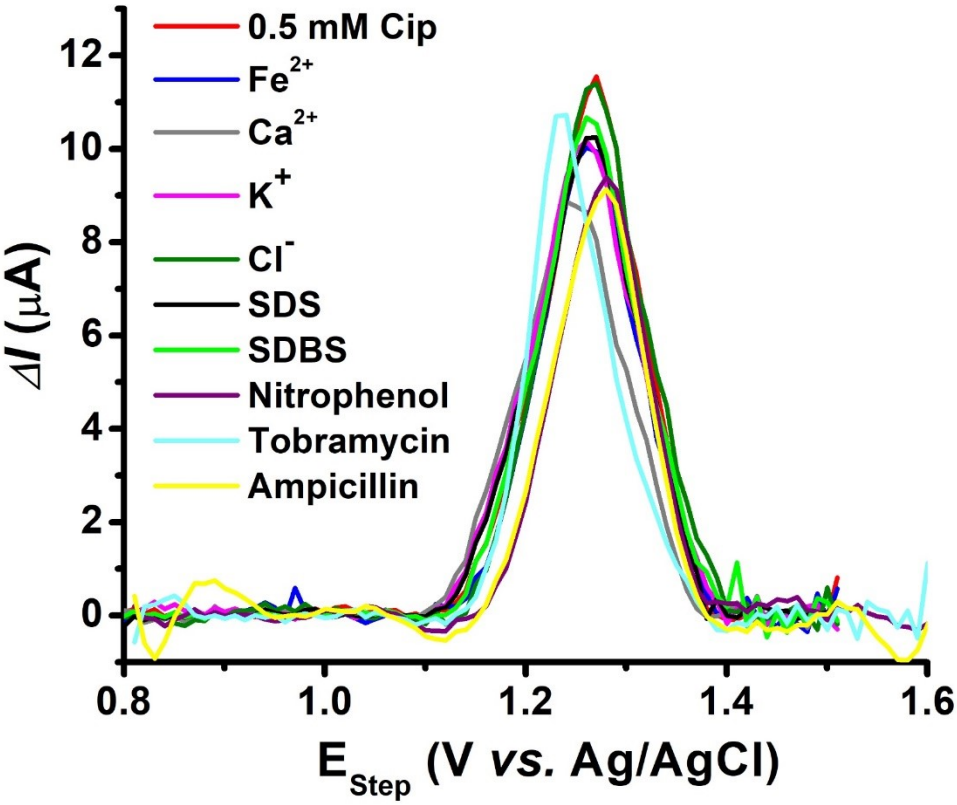

Fig. S10. SWV collected in the presence of possible interference species (1 mM) purposefully added to 0.1 M $NaNO_3$, containing 0.5 mM Cip.

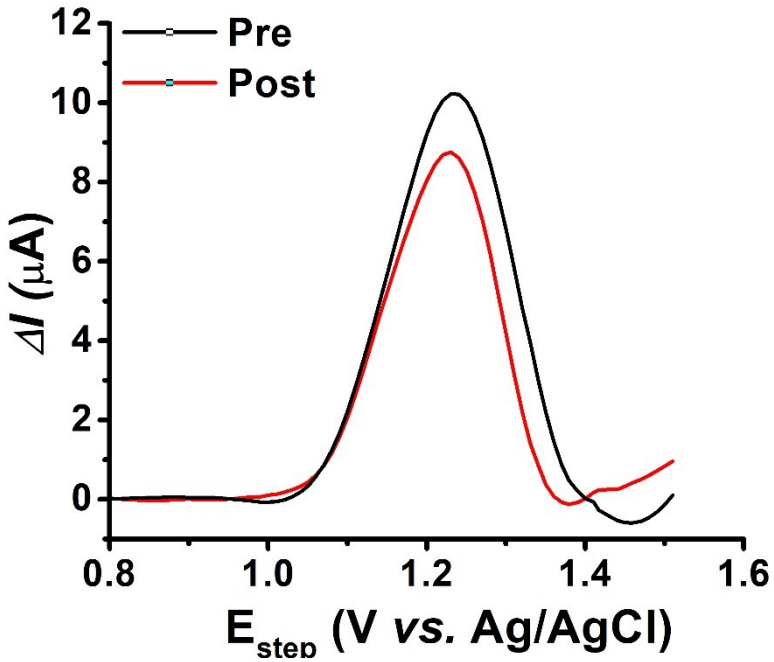

Fig. 11. SWV acquired before and after stability measurements (100 cycles of CV at 50 mV s^{-1})

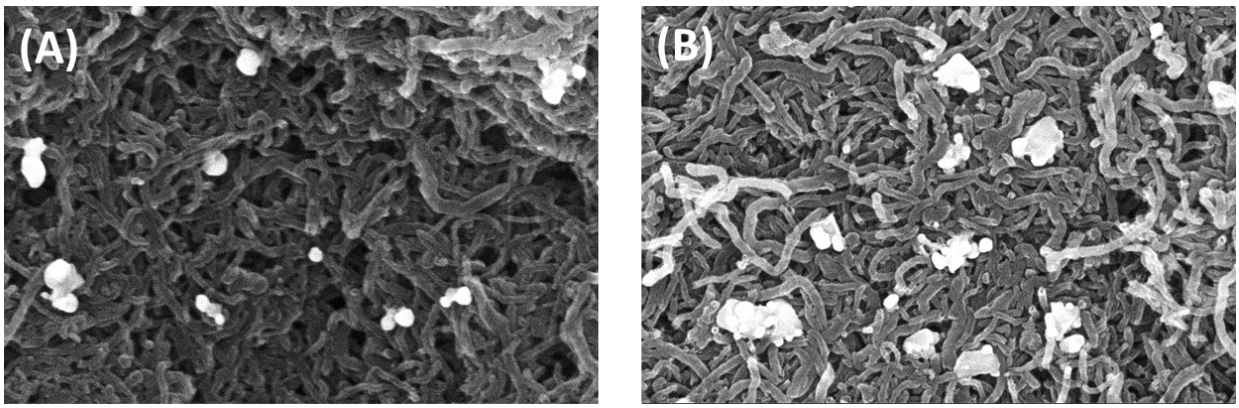

Fig. S12. SEM images of the sensor surface before (E) and after 100 CV cycles (F) for stability analysis at the OCNTs-PDA-Ag sensor

Reference:

1 P. Gayen and B. P. Chaplin, *ACS Appl. Mater. Interfaces*, 2016, **8**, 1615–1626.

2 A. Tiwari, V. Singh, D. Mandal and T. C. Nagaiah, *J. Mater. Chem. A*, 2017, **5**, 20014–20023.

3 V. Singh and T. C. Nagaiah, *J. Mater. Chem. A*, 2019, **7**, 10019–10029.

4 G. Loget, J. B. Wood, K. Cho, A. R. Halpern and R. M. Corn, *Anal. Chem.*, 2013, **85**, 9991–9995.

5 A. Tiwari and T. C. Nagaiah, *ChemCatChem*, 2016, **8**, 396–403.

6 G. S. Garbellini, R. C. Rocha-Filho and O. Fatibello-Filho, *Anal. Methods*, 2015, **7**, 3411–3418.

7 P. Gayen and B. P. Chaplin, *ACS Appl. Mater. Interfaces*, 2016, **8**, 1615–1626.

8 A. Pollap, K. Baran, N. Kuszewska and J. Kochana, *J. Electroanal. Chem.*, , DOI:10.1016/j.jelechem.2020.114574.

9 T. S. H. Pham, P. J. Mahon, G. Lai and A. Yu, *Electroanalysis*, 2018, **30**, 2185–2194.

10 J. M. P. J. Garrido, M. Melle-Franco, K. Strutyński, F. Borges, C. M. A. Brett and E. M. P. J. Garrido, *J. Environ. Sci. Heal. Part A*, 2017, **52**, 313–319.

11 X. Fang, X. Chen, Y. Liu, Q. Li, Z. Zeng, T. Maiyalagan and S. Mao, *ACS Appl. Nano Mater.*, 2019, **2**, 2367–2376.

12 Y. Yuan, F. Zhang, H. Wang, L. Gao and Z. Wang, *ECS J. Solid State Sci. Technol.*, 2018, **7**, M201–M208.

13 H. B. Lee, T. E. Peart and M. L. Svoboda, *J. Chromatogr. A*, 2007, **1139**, 45–52.

14 S. S. Wu, C. Y. Chein and Y. H. Wen, *J. Chromatogr. Sci.*, 2008, **46**, 490–495.